

Synthesis, Crystal Structures, and Photophysical Properties of Homodinuclear Lanthanide Xanthene-9-carboxylates

R. Shyni,[†] S. Biju,[†] M. L. P. Reddy,^{*†} Alan H. Cowley,[‡] and Michael Findlater[‡]

Chemical Sciences and Technology Division, National Institute for Interdisciplinary Science & Technology (NIIST), Thiruvananthapuram-695 019, India, and Department of Chemistry and Biochemistry, The University of Texas at Austin, 1 University Station A5300, Austin, Texas 78712

Received June 1, 2007

Three new homodinuclear lanthanide(III) complexes of xanthene-9-carboxylic acid, $[\text{Ln}_2(\text{XA})_6(\text{DMSO})_2(\text{H}_2\text{O})_2](\text{Ln} = \text{Eu} \text{ (1)}, \text{Tb} \text{ (2)} \text{ and } \text{Gd} \text{ (3)}; \text{HXA} = \text{xanthene-9-carboxylic acid}; \text{DMSO} = \text{dimethylsulfoxide})$, have been synthesized, of which **1** and **2** were structurally characterized by single-crystal X-ray diffraction. These compounds crystallize in the monoclinic space group $P2_1/n$ with $a = 17.849(4) \text{ \AA}$, $b = 9.6537(19) \text{ \AA}$, $c = 23.127(5) \text{ \AA}$, $\beta = 109.06(3)^\circ$, and $V = 3766.5(13) \text{ \AA}^3$ for **1** and $a = 17.809(4) \text{ \AA}$, $b = 9.6548(19) \text{ \AA}$, $c = 23.075(5) \text{ \AA}$, $\beta = 108.97(3)^\circ$, and $V = 3752.1(13) \text{ \AA}^3$ for **2**. The crystal structures of **1** and **2** consist of homodinuclear species that are bridged by two oxygen atoms from two carboxylate ligands. The two lanthanide ions are related by a center of inversion. Each lanthanide ion is coordinated by eight oxygen atoms in an overall distorted square-prismatic geometry. Six of the oxygen atoms are furnished by the carboxylate moieties, and the remaining two oxygen atoms are provided by water and DMSO molecules. The photophysical properties of these complexes in the solid state at room temperature have been investigated. The quantum yields were found to be 0.06 ± 0.01 and $7.30 \pm 0.73\%$ for **1** and **2**, respectively.

Introduction

Lanthanide complexes have long been known to give sharp, intense emission lines upon irradiation with ultraviolet light due to intramolecular energy transfer from the coordinated ligands to the luminescent central lanthanide ion, which, in turn, undergoes the corresponding radiative process (the so-called antenna effect).¹ Thus, these complexes have been employed for a wide range of photonic applications such as tunable lasers, amplifiers for optical communications, components of emitting materials in multilayer organic light-emitting diodes, and luminescent probes for analytes.¹ Because the Laporte-forbidden $4f-4f$ transition prevents direct excitation of lanthanide luminescence, these metal ions

require sensitization by suitable organic chromophores.² Furthermore, for practical applications under physiological conditions, it is important to incorporate the lanthanides into water stable coordination complexes. Recently, aromatic carboxylate coordination complexes that exhibit unique photophysical properties and intriguing structural features have attracted considerable interest.³ For example, a series of benzoic acid derivatives have been evaluated as possible sensitizers for Eu(III) and Tb(III) luminescence.⁴ Several complexes of Eu^{3+} and Tb^{3+} with *o*-, *m*-, and *p*-nitrobenzoic acid have also been synthesized, and their photophysical properties have been investigated both in the solid state and in methanol solution.^{4a} All of the compounds exhibit weak luminescence in the solid state and moderate quantum yields in methanol solution (1 and 3% for Eu^{3+} and Tb^{3+} ,

* To whom correspondence should be addressed. E-mail: mlpreddy@yahoo.co.uk.

[†] National Institute for Interdisciplinary Science and Technology.

[‡] University of Texas at Austin.

(1) (a) Lehn, J.-M. *Angew. Chem., Int. Ed. Engl.* **1990**, *29*, 1304–1319. (b) de Sa, G. F.; Malta, O. L.; de Mello Donega, C.; Simas, A. M.; Longo, R. L.; Santa-Cruz, P. A.; da Silva, E. F., Jr. *Coord. Chem. Rev.* **2000**, *196*, 165–195. (c) Kido, J.; Okamoto, Y. *Chem. Rev.* **2002**, *102*, 1257–2368. (d) Bunzli, J.-C. G.; Piguet, C. *Chem. Soc. Rev.* **2005**, *34*, 1048–1077. (e) Bunzli, J.-C. G.; Piguet, C. *Chem. Rev.* **2002**, *102*, 1897–1928. (f) Parker, D. *Coord. Chem. Rev.* **2000**, *205*, 109–130.

(2) Chatterton, N.; Bretonniere, Y.; Pecaut, J.; Mazzanti, M. *Angew. Chem., Int. Ed.* **2005**, *44*, 7595–7598.

(3) (a) Eddaudi, M.; Kim, J.; Wachter, J. B.; Chae, H. K.; O' Keeffe, M.; Yaghi, O. M. *J. Am. Chem. Soc.* **2001**, *123*, 4368–4369. (b) Pan, L.; Sander, M. B.; Huang, X.; Li, J.; Smith, M.; Bittner, E.; Bockrath, B.; Johnson, J. K. *J. Am. Chem. Soc.* **2004**, *126*, 1308–1309. (c) Chen, X. Y.; Bretonniere, Y.; Pecaut, J.; Imbert, D.; Bunzli, J. C. G.; Mazzanti, M. *Inorg. Chem.* **2007**, *46*, 625–637. (d) Teotonio, E. E. S.; Felinto, M. C. F. C.; Brito, H. F.; Malta, O. L.; Trindade, A. C.; Najjar, R.; Streck, W. *Inorg. Chim. Acta.* **2004**, *357*, 451–460.

respectively). Subsequently, it has been reported that thiophenyl-derivatized nitrobenzoic acid is a superior sensitizer for Eu^{3+} and Tb^{3+} .^{4b} The strong fluorescent emissions of homodinuclear lanthanide complexes of 4-cyanobenzoic acid demonstrate that ligand-to-Ln(III) energy transfer is efficient and that coordinated water molecules do not quench the luminescence by nonradiative dissipation of energy.⁵ The enhancement of terbium-centered luminescence through thiophene derivatization of isophthalic acid has also been well documented.⁶ Typical examples of lanthanide carboxylate complexes that can be incorporated into electroluminescent devices include $\text{Tb}(\text{AHBA})_3$ (AHBA = 2-amino-4-hexadecylbenzoic acid),⁷ $\text{Tb}(\text{MeOBB})_3$ (MeOBB = 2-(4-methoxybenzoyl)benzoic acid), and $\text{Eu}(\text{MeOBB})_3$.⁸

Given the important potential applications of lanthanide carboxylates and the fascinating properties of these ligands, we were prompted to prepare a new series of lanthanide complexes featuring the xanthene-9-carboxylate ligand. Herein, we describe the syntheses and photophysical properties of the homodinuclear xanthene-9-carboxylate complexes of Eu^{3+} , Tb^{3+} , and Gd^{3+} . The Eu and Tb complexes were structurally characterized by single-crystal X-ray diffraction.

Experimental Section

Materials and Instrumentation. The commercially available chemicals Eu(III) nitrate hexahydrate (99.9%, Acros Organics), Gd(III) nitrate hexahydrate (99.9%, Acros Organics), Tb(III) nitrate hexahydrate (99.9%, Acros Organics), and xanthene-9-carboxylic acid (98%, Aldrich) were used without further purification. All of the other chemicals used were of analytical reagent grade.

Elemental analyses were performed with a PerkinElmer Series 2 Elemental Analyzer 2400. A Nicolet FTIR 560 Magna Spectrometer using KBr (neat) was used to obtain the IR spectral data, and a Bruker 300 MHz NMR spectrometer was used for the acquisition of ^1H NMR spectral data in $\text{DMSO}-d_6$ solution. Thermogravimetric analyses were carried out using a TGA-50H instrument (Shimadzu, Japan). The diffuse reflectance spectra of the new lanthanide complexes and the standard phosphor were recorded on a Shimadzu, UV-2450 UV-vis spectrophotometer using BaSO_4 as a reference. The absorbances of the ligands and the corresponding complexes were measured in DMSO solution on a UV-vis spectrophotometer (Shimadzu, UV-2450). The photoluminescence (PL) spectra were recorded using a Spex-Fluorolog DM3000F spectrofluorometer with a double grating, 0.22 m Spex 1680 monochromators, and a 450W xenon lamp as the excitation source (front-face mode). The excitation and emission

spectra of the complexes were corrected for instrumental function. The lifetime measurements were carried out at room temperature using a Spex 1934 D phosphorimeter.

The overall quantum yields (Φ_{overall}) were measured at room temperature using the technique for powdered samples described by Bril et al.,^{9a} and the following expression

$$\phi_{\text{overall}} = \left(\frac{1 - r_{\text{st}}}{1 - r_{\text{x}}} \right) \left(\frac{A_{\text{x}}}{A_{\text{st}}} \right) \Phi_{\text{st}} \quad (1)$$

where r_{st} and r_{x} represent the diffuse reflectance (with respect to a fixed wavelength) of the complexes and of the standard phosphor, respectively, and Φ_{st} is the quantum yield of the standard phosphor. The terms A_{x} and A_{st} represent the areas under the complex and the standard emission spectra, respectively. To acquire absolute intensity values, BaSO_4 was used as a reflecting standard. The standard phosphor used was sodium salicylate (Merck), the emission spectrum of which comprises an intense broad band with a maximum at approximately 425 nm, and a constant Φ value (60%) for excitation wavelengths between 220 and 380 nm. Three measurements were carried out for each sample, and the reported Φ_{overall} value corresponds to the arithmetic mean value of the three values. The errors in the quantum yield values associated with this technique were estimated to be $\pm 10\%$.⁹

The X-ray diffraction data were collected at 153 K on a Nonius Kappa CCD diffractometer equipped with an Oxford Cryostream low-temperature device and a graphite-monochromated $\text{Mo K}\alpha$ radiation source ($\lambda = 0.71073 \text{ \AA}$). Corrections were applied for Lorentz and polarization effects. All of the structures were solved by direct methods¹⁰ and refined by full-matrix least-squares cycles on F^2 . All of the nonhydrogen atoms were allowed anisotropic thermal motion, and the hydrogen atoms were placed in fixed, calculated positions using a riding model (C–H, 0.96 \AA). Selected crystal data and data collection and refinement parameters are listed in Table 1. Selected metrical parameters are presented in Table 2. X-ray crystallographic information files can be obtained free of charge via www.ccdc.cam.ac.uk/const/retrieving.html (or from CCDC, 12 Union Road, Cambridge CB2 1EZ, U.K.; fax +44 1223 336033; e-mail deposit @ccdc.cam.ac.uk). CCDC 659663 for **1** and CCDC 659664 for **2** in this article.

Synthesis of Homodinuclear Complexes. An aqueous solution of $\text{Ln}(\text{NO}_3)_3 \cdot 6\text{H}_2\text{O}$ (0.5 mmol) (Ln = Eu, Tb, or Gd) was added to a solution of xanthene-9-carboxylic acid (1.5 mmol) in water in the presence of NaOH (1.5 mmol). Precipitation took place immediately, and each reaction mixture was stirred subsequently for 10 h at room temperature¹¹ (Scheme 1). The product was filtered, washed with water, dried, and stored in a desiccator. The resulting complexes were then purified by recrystallization from a dimethylsulfoxide/tetrahydrofuran solvent mixture. Single crystals were obtained from a dimethylsulfoxide/tetrahydrofuran solvent mixture after storage for three weeks at ambient temperature.

$\text{Eu}_2(\text{XA})_6(\text{DMSO})_2(\text{H}_2\text{O})_2$ (1**).** Elemental analysis: Calcd for $\text{C}_{88}\text{H}_{70}\text{Eu}_2\text{O}_{22}\text{S}_2$ (1847.56): C, 57.20; H, 3.81; S, 3.47. Found: C, 57.11; H, 3.67; S, 3.32. IR (KBr) ν_{max} : 3434, 1602, 1572, 1541, 1479, 1454, 1391, 1259, 1116, 1040, 949, 749 cm^{-1} .

- (4) (a) de Bettencourt-Dias, A.; Viswanathan, S. *Dalton Trans.* **2006**, 34, 4093–4103. (b) Viswanathan, S.; de Bettencourt-Dias, A. *Inorg. Chem.* **2006**, 45, 10138–10146. (c) Fiedler, T.; Hilder, M.; Junk, P. C.; Kynast, U. H.; Lezhnina, M. M.; Warzala, M. *Eur. J. Inorg. Chem.* **2007**, 2, 291–301. (d) Soares-Santos, P. C. R.; Nogueira, H. I. S.; Paz, F. A. A.; Ferreira, R. A. S.; Carlos, L. D.; Klinowski, J.; Trindade, T. *Eur. J. Inorg. Chem.* **2003**, 19, 3609–3617. (e) Lam, A. W. H.; Wong, W. T.; Gao, S.; Wen, G.; Zhang, X. X. *Eur. J. Inorg. Chem.* **2003**, 1, 149–163. (f) Li, X.; Zhang, Z. Y.; Zou, Y. Q. *Eur. J. Inorg. Chem.* **2005**, 14, 2909–2918.
- (5) Li, Y.; Zheng, F. K.; Liu, X.; Zou, W. Q.; Guo, G. C.; Lu, C. Z.; Huang, J. S. *Inorg. Chem.* **2006**, 45, 6308–6316.
- (6) de Bettencourt-Dias, A. *Inorg. Chem.* **2005**, 44, 2734–2741.
- (7) Zheng, Y. X.; Shi, C. Y.; Liang, Y. J.; Lin, Q.; Guo, C.; Zhang, H. J. *Synth. Met.* **2000**, 114, 321–323.
- (8) Edward, A.; Claude, C.; Sokolik, I.; Chu, T. Y.; Okamoto, Y.; Dorsinville, R. *J. Appl. Phys.* **1997**, 82, 1841–1846.

- (9) (a) Bril, A.; De Jager-Veenis, A. W. *J. Electrochem. Soc.* **1976**, 123, 396–398. (b) Mello Donega, C. D.; Junior, S. A.; de Sa, G. F. *Chem. Commun.* **1996**, 11, 1199–1200. (c) Carlos, L. D.; Mello Donega, C. D.; Albuquerque, R. Q.; Junior, S. A.; Menezes, J. F. S.; Malta, O. L. *Mol. Phys.* **2003**, 101, 1037–1045.
- (10) Sheldrick, G. M., *SHELL-PC*, version 5; Siemens Analytical X-ray Instruments, Inc.: Madison, WI, U.S.A., 1994.
- (11) Zhang, Z.; Wan, S.; Okamura, T.; Sun, W.; Ueyama, N. *Z. Anorg. Allg. Chem.* **2006**, 632, 679–683.

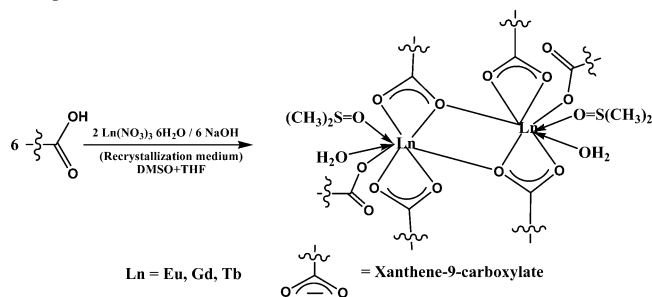
Table 1. Crystal Data, Collection, and Structure Refinement Parameters for **1** and **2**

parameters	1	2
empirical formula	C ₄₄ H ₃₃ EuO ₁₁ S	C ₄₄ H ₃₃ TbO ₁₁ S
fw	921.72	928.68
cryst syst	monoclinic	monoclinic
space group	<i>P2₁/n</i>	<i>P2₁/n</i>
cryst size (mm ³)	0.20 × 0.15 × 0.15	0.25 × 0.25 × 0.15
temperature (K)	153(2)	153(2)
<i>a</i> (Å)	17.849(4)	17.809(4)
<i>b</i> (Å)	9.6537(19)	9.6548(19)
<i>c</i> (Å)	23.127(5)	23.075(5)
α (deg)	90	90
β (deg)	109.06(3)	108.97(3)
γ (deg)	90	90
<i>V</i> (Å ³)	3766.5(13)	3752.1(13)
<i>Z</i>	4	2
ρ _{calcd} (g cm ⁻³)	1.625	1.644
μ (mm ⁻¹)	1.786	2.006
<i>F</i> (000)	1856	1864
R1 [<i>I</i> > 2σ(<i>I</i>)]	0.0437	0.0457
wR2 [<i>I</i> > 2σ(<i>I</i>)]	0.0900	0.1005
R1 (all data)	0.0949	0.0965
wR2 (all data)	0.1215	0.1317
GOF	1.034	1.022

Table 2. Selected Bond Lengths and Bond Angles for **1** and **2**

	1	2	
Eu1–Eu1 ₃ ^a	4.1081(8)	Tb1–Tb1 ₃ ^a	4.076(1)
Eu1–O1	2.531(3)	Tb1–O1	2.522(7)
Eu1–O2	2.424(3)	Tb1–O2	2.409(7)
Eu1–O3	2.249(3)	Tb1–O5	2.591(6)
Eu1–O5	2.379(3)	Tb1–O4	2.462(6)
Eu1–O5#1	2.609(3)	Tb1–O5#1	2.357(6)
Eu1–O6	2.402(3)	Tb1–O7	2.242(6)
Eu1–O7	2.475(3)	Tb1–O10	2.352(6)
Eu1–O9	2.367(3)	Tb1–O11	2.388(7)
O3–Eu1–O9	78.60(12)	O7–Tb1–O10	78.4(2)
O9–Eu1–O6	78.25(12)	O10–Tb1–O11	78.3(2)
O6–Eu1–O5#1	71.47(11)	O11–Tb1–O5#1	82.6(2)
O5–Eu1–O5#1	69.20(12)	O5–Tb1–O5#1	69.1(2)
O5–Eu1–O7	120.26(11)	O5–Tb1–O4	51.56(19)
O7–Eu1–O2	77.03(12)	O4–Tb1–O2	76.9(2)
O2–Eu1–O1	52.26(11)	O2–Tb1–O1	52.4(2)
O1–Eu1–O3	84.95(12)	O1–Tb1–O7	84.6(2)

^a Eu1 and Eu1₃ and Tb1 and Tb1₃ are symmetrical metal atoms.

Scheme 1. Synthetic Route to the Homobimetallic Lanthanide Complexes

Tb₂(XA)₆(DMSO)₂(H₂O)₂ (2**).** Elemental analysis: Calcd for C₈₈H₇₀Tb₂O₂₂S₂ (1861.48): C, 56.78; H, 3.79; S, 3.44. Found: C, 56.66; H, 3.88; S, 3.35. IR (KBr) ν_{max}: 3351, 1602, 1572, 1542, 1483, 1453, 1405, 1260, 1034, 949, 748 cm⁻¹.

Gd₂(XA)₆(DMSO)₂(H₂O)₂ (3**).** Elemental analysis (%): Calcd for C₈₈H₇₀Gd₂O₂₂S₂ (1858.02): C, 56.88; H, 3.79; S, 3.45. Found: C, 56.47; H, 3.41; S, 3.41. IR (KBr) ν_{max}: 3395, 1603, 1571, 1545, 1485, 1453, 1387, 1319, 1261, 1119, 1038, 874, 749 cm⁻¹.

Results and Discussion

Synthesis and Characterization of Complexes 1–3. The synthetic procedure for Ln³⁺ complexes **1–3** is summarized in Scheme 1. The elemental analysis data for **1–3** reveal that each Ln³⁺ ion has reacted with HXA in a metal-to-ligand mole ratio of 1:3. The carbonyl stretching frequencies for **1–3** appear at lower energies than that for HXA (1688 cm⁻¹), indicating that the carbonyl oxygen atoms are coordinated to the Ln³⁺ ion in each case. Furthermore, the IR spectra of **1–3** show three different values for the carbonyl stretching frequency (for **1**: 1602, 1572, 1541 cm⁻¹; **2**: 1602, 1572, 1542 cm⁻¹; **3**: 1603, 1571, 1545 cm⁻¹) due to the fact that the xanthene-9-carboxylate ligands exhibit three different coordination modes (vide infra). The broad IR band that is apparent in the 3000–3500 cm⁻¹ region for **1–3** is indicative of the presence of coordinated water molecules in these complexes. Likewise, the peaks detected in the ~1030–1040 cm⁻¹ region imply the presence of coordinated DMSO molecules in these complexes. These peaks are red-shifted with respect to that of unligated DMSO (1047 cm⁻¹). It is clear from the thermogravimetric analysis data that **1–3** (Figure S1 in the Supporting Information) undergo a mass loss of 11% (Calcd: 10.3%) up to 275 °C, which corresponds to the elimination of the coordinated solvent molecules. Further decomposition takes place in two steps, the first of these occurring between 275 and 350 °C (59% mass loss for **1**, 60% for **2**, and 57% for **3**) and the second between 350 and 600 °C (10% mass loss for **1**, 9% for **2**, and 12% for **3**), leaving a residue of approximately 20% for **1–3**, which corresponds to the lanthanide oxides.

X-ray Structural Characterization. The structures of Eu₂(XA)₆(DMSO)₂(H₂O)₂ (**1**) and Tb₂(XA)₆(DMSO)₂(H₂O)₂ (**2**) were determined by single-crystal X-ray diffraction. Details of the crystal data and data collection parameters are given in Table 1, and selected bond lengths and bond angles are listed in Table 2. **1** and **2** are isostructural and crystallize in the monoclinic space group *P2₁/n*. Each complex molecule is dimeric, containing two Ln³⁺ ions, surrounded by six xanthene-9-carboxylate ligands. The dimeric structure features an inversion center of symmetry indicating that the Ln(1) and Ln(1₃) centers are in equivalent chemical environments. The Ln–Ln distances are 4.108 Å (**1**) and 4.076 Å (**2**). A comparison with structures that are available in the CSD¹² reveals that this distance falls within the range of 3.785–4.532 Å that has been observed for Ln³⁺ complexes that feature the bridging bidentate coordination mode. The ligands show three different coordination modes to the Ln ions: bidentate chelating, tridentate chelating bridging, and monodentate, thus corroborating the IR data. The coordination environment for **1** is shown in part (b) of Figure 1 for **1** and is representative of both complexes. The atoms O(1) and O(2) belong to the carboxylate ligand, which binds in a bidentate fashion to the Eu(1) ion. One carboxylate group bridges the two Eu ions in a triply coordinated manner. The other carboxylate group, O(3), binds in a monodentate mode. The coordination sphere of the metal ion is completed by

(12) Cambridge Structural Database, version 5.27.; <http://www.ccdc.ac.uk>.

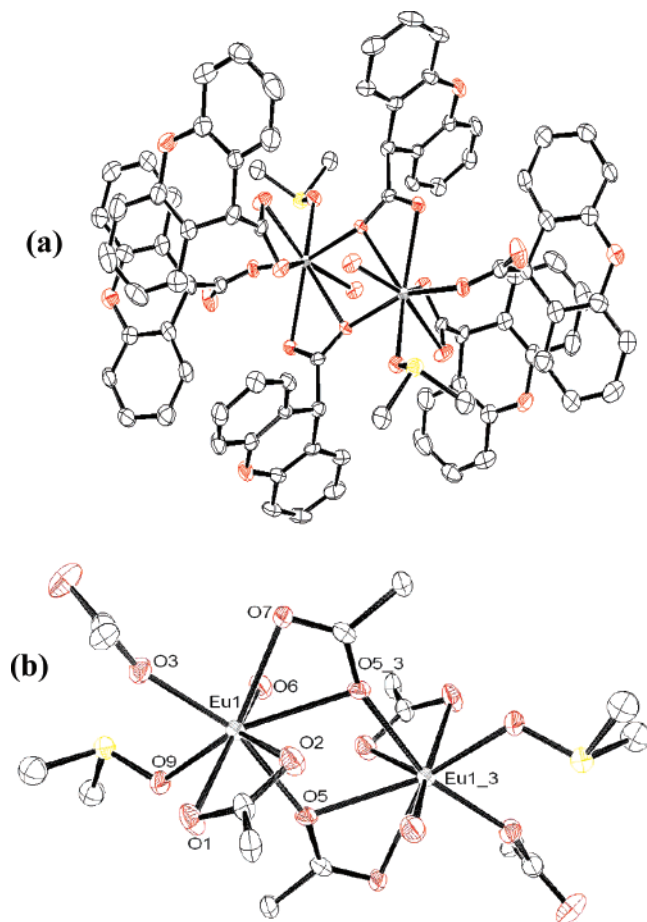


Figure 1. (a) ORTEP diagram for **1**, (b) Coordination environment of the Eu^{3+} ions in **1** with partial atom-labeling scheme. All of the hydrogen atoms were omitted for clarity. Eu1 and Eu1_3 are symmetrical metal atoms.

water and DMSO molecules bonding via O(6) and O(9), producing a coordination number of eight at the Eu^{3+} center. The coordination polyhedra can be described as distorted square antiprisms of approximately C_{2v} symmetry in which six oxygen atoms belong to the three xanthene-9-carboxylate moieties and two oxygen atoms are provided by one water and one DMSO molecule. In **1**, the Eu–O bond lengths range from 2.249 to 2.609 Å, and in **2** the Tb–O bond lengths are in the range of 2.242 to 2.591 Å (Figure S2 in the Supporting Information), which fall in the expected range for this type of complex.^{4c} The longest Eu–O bonds involve the oxygen atoms of one of the triply coordinated ligands [Eu(1)–O(5) = 2.609 Å, Eu(1)–O(7) = 2.475 Å] and the shortest such bond is associated with the monodentate carboxylate ligand [Eu(1)–O(3) = 2.249 Å]. On the other hand, the Eu–O distances of the coordinated water and DMSO molecules [Eu(1)–O(6) = 2.402 Å and Eu(1)–O(9) = 2.367 Å, respectively] are shorter than those of the bidentate and tridentate xanthates. It is interesting to note that, due to the coordination of H_2O and DMSO molecules, one of the terminal carboxylate groups on each Ln center ligates in a monodentate fashion. Similar trends in bond lengths and intermetallic distances have been reported by Viswanathan and Bettencourt-Dias for dimeric Eu^{3+} and Tb^{3+} complexes of thiophenyl-derivatized nitrobenzoate ligands.^{4b}

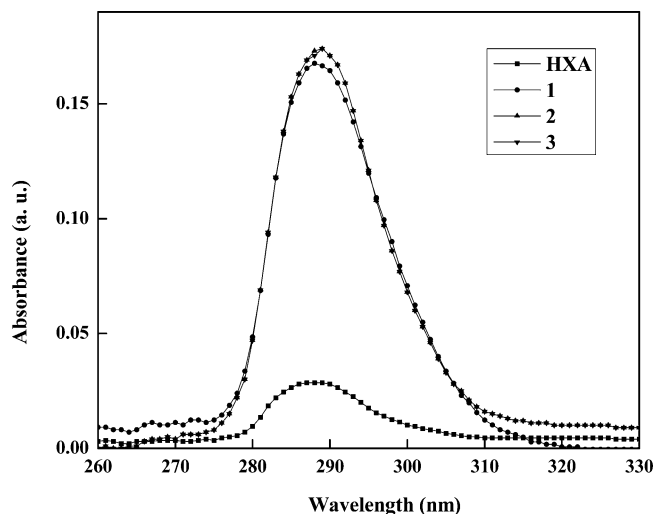


Figure 2. UV–vis absorption spectra of xanthene-9-carboxylic acid (HXA) and **1–3** in DMSO solution ($c = 1 \times 10^{-5}$ M).

UV–Vis Spectra. The UV–vis absorption spectra of the free ligand HXA and the corresponding xanthate Ln^{3+} complexes were measured in DMSO solution ($c = 1 \times 10^{-5}$ M), and are displayed in Figure 2. The absorption maxima for **1** (290 nm), **2** (290 nm), and **3** (289 nm), which are attributable to singlet–singlet ${}^1\pi\text{--}\pi^*$ absorptions of the aromatic rings, are slightly red-shifted with respect to that of the free ligand HXA ($\lambda_{\text{max}} = 287$ nm). The shapes of the spectral bands for the complexes are similar to that of the free ligand, suggesting that the coordination of the Ln^{3+} ion does not have a significant influence on the ${}^1\pi\text{--}\pi^*$ transition. However, a small red shift observed in the absorption maximum of each complex is a consequence of the enlargement of the conjugate structure of the ligands after coordination to the lanthanide ion. The molar absorption coefficient values (ϵ) for **1–3** at λ_{max} are 1.67×10^4 , 1.74×10^4 , and 1.69×10^4 $\text{L mol}^{-1} \text{cm}^{-1}$, respectively, which are about six times than that of HXA (2.85×10^3 $\text{L mol}^{-1} \text{cm}^{-1}$ at 287 nm), indicating the presence of six xanthate ligands per homodinuclear lanthanide complex. Furthermore, the large molar absorption coefficient for HXA indicates that the carboxylic acid ligand has a strong ability to absorb light.

PL Properties of Complexes 1 and 2. The normalized steady-state excitation and emission spectrum of homodinuclear europium complex **1** (in the solid state) at room temperature is shown in Figure 3. The excitation spectrum of **1** exhibits a series of sharp lines characteristic of the Eu^{3+} energy-level structure, and can be assigned to transitions between the ${}^7\text{F}_{0,1}$ and ${}^5\text{L}_6$, ${}^5\text{D}_{3,2,1}$ levels.¹³ A weak, broad band between 250 and 450 nm is also evident. This transition is less intense than the 4f absorption of the europium ion, which proves that luminescence sensitization via excitation of the ligand is not efficient in **1**. The ambient temperature emission

(13) (a) Carnall, W. T. In *Handbook on the Physics and Chemistry of Rare Earths*; Gschneidner, K. A., Eyring, L., Eds.; Elsevier: Amsterdam, The Netherlands, 1987; Vol. 3, Chapter 24, pp 171–208. (b) Dieke, G. H. *Spectra and Energy Levels of Rare Earth Ions in Crystals*; Interscience: New York, 1968. (c) Biju, S.; Ambili Raj, D. B.; Reddy, M. L. P.; Kariuki, B. M. *Inorg. Chem.* **2006**, *45*, 10651–10660.

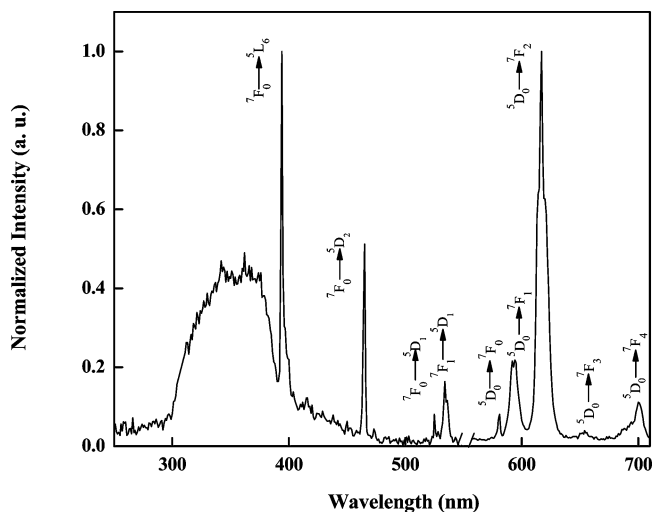


Figure 3. Room-temperature (300 K) excitation and emission spectra for **1** ($\lambda_{\text{ex}} = 362$ nm) with emissions monitored at approximately 613 nm.

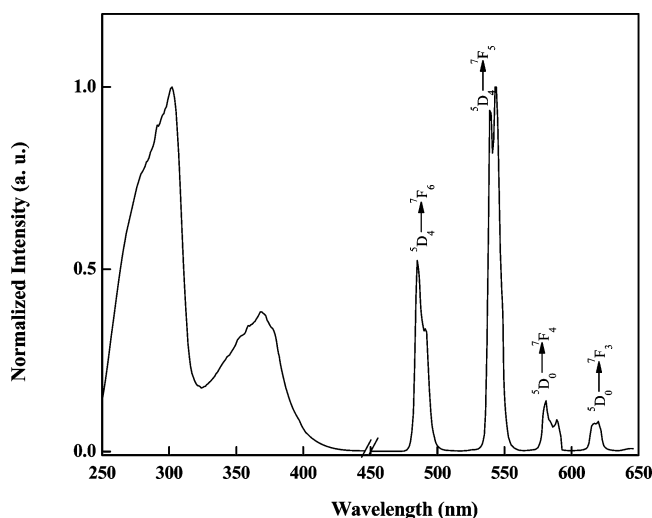


Figure 4. Room-temperature (300 K) excitation and emission spectra for **2** ($\lambda_{\text{ex}} = 302$ nm) with emissions monitored at approximately 545 nm.

spectrum of **1** ($\lambda_{\text{ex}} = 362$ nm) displays characteristically sharp peaks in the 575–725 nm region, which are associated with the ${}^5\text{D}_0 \rightarrow {}^7\text{F}_{0-4}$ transitions of the Eu^{3+} ion.^{13,14} The five peaks that are anticipated for the ${}^5\text{D}_0 \rightarrow {}^7\text{F}_{0-4}$ transitions are well resolved, and the hypersensitive ${}^5\text{D}_0 \rightarrow {}^7\text{F}_2$ transition is very intense, pointing to a highly polarizable chemical environment around the Eu^{3+} ion. The presence of only one line for the ${}^5\text{D}_0 \rightarrow {}^7\text{F}_0$ transition strongly indicates the existence of only one coordination site for the Eu^{3+} cations, as this transition occurs between nondegenerated levels.

The excitation spectrum of terbium complex **2**, monitored around the peak of the intense ${}^5\text{D}_4 \rightarrow {}^7\text{F}_5$ transition of the Tb^{3+} ion, exhibits a broad band between 250 and 450 nm with a maximum at approximately 302 and a shoulder at 360 nm (Figure 4). The peak at 302 nm can be assigned to the ${}^1\pi-\pi^*$ transition of the aromatic ring, and the shoulder at 360 nm is attributable to the ${}^1\pi-\pi^*$ transition of the

carbonyl group of the HXA ligand. The room-temperature normalized emission spectra of terbium complex **2** exhibit the characteristic emission bands for Tb^{3+} ($\lambda_{\text{ex}} = 302$ nm) centered at 490, 545, 585, and 620 nm, which result from deactivation of the ${}^5\text{D}_4$ excited state to the corresponding ground state ${}^7\text{F}_J$ ($J = 6, 5, 4, 3$) of the Tb^{3+} ion (Figure 4). The most-intense emission is centered at 545 nm and corresponds to the hypersensitive transition ${}^5\text{D}_4 \rightarrow {}^7\text{F}_{5,13a,13b,15}$.

The overall quantum yield (Φ_{overall}) for a lanthanide complex treats the system as a black box in which the internal process is not explicitly considered. Given that the complex absorbs a photon (i.e., the antenna is excited), the overall quantum yield can be defined as¹⁶

$$\Phi_{\text{overall}} = \Phi_{\text{transfer}} \Phi_{\text{Ln}} \quad (2)$$

Here, Φ_{transfer} is the efficiency of energy transfer from the ligand to Ln^{3+} , and Φ_{Ln} represents the intrinsic quantum yield of the lanthanide ion. The overall quantum yields (Φ_{overall}) for lanthanide complexes **1** and **2** were found to be 0.06 ± 0.01 and $7.30 \pm 0.73\%$, respectively. The lifetime value for the ${}^5\text{D}_4$ level of **2** ($\tau = 1.11 \pm 0.01$ ms) was determined from the luminescence decay profile at room temperature by fitting with a monoexponential curve. A typical decay profile for **2** is shown in Figure S3 (in the Supporting Information). On the other hand, a shorter lifetime was observed for **1** ($\tau = <10$ μs). The observed quantum yield and lifetime values, especially those for the homodinuclear terbium complex, were found to be promising, as compared to those reported recently for a homodinuclear terbium complex of nitrobenzoic acid ($\Phi = 3.14\%$ and $\tau = 666.7 \pm 28.5$ μs in methanol solution)^{4a} and a homodinuclear terbium complex of thiophene carboxylic acid ($\tau = 230$ μs in solid state).^{3d}

Energy Transfer between the Ligand and Ln^{3+} . To demonstrate the energy transfer process, the phosphorescence spectrum of $\text{Gd}_2(\text{XA})_6(\text{DMSO})_2(\text{H}_2\text{O})_2$ was measured for the triplet energy-level data of HXA. From the phosphorescence spectra (Figure 5), the triplet energy level (${}^3\pi\pi^*$) of $\text{Gd}_2(\text{XA})_6(\text{DMSO})_2(\text{H}_2\text{O})_2$, which corresponds to its lower wavelength emission edge, is $25\,839$ cm^{-1} (387 nm). Because the lowest excited state, ${}^6\text{P}_{7/2}$, of Gd^{3+} is too high to accept energy from the ligand, the data obtained from the phosphorescence spectra actually reveal the triplet energy level of HXA in lanthanide complexes.¹⁷ The singlet state energy (${}^1\pi\pi^*$) level of HXA is estimated by referencing its absorbance edge, which is $32\,573$ cm^{-1} (307 nm).

In general, the sensitization pathway in luminescent europium complexes consists of excitation of the ligands into

(14) (a) Pavithran, R.; Saleesh Kumar, N. S.; Biju, S.; Reddy, M. L. P.; Alves, S., Jr.; Freire, R. O. *Inorg. Chem.* **2006**, *45*, 2184–2192. (b) Pavithran, R.; Reddy, M. L. P.; Alves, S., Jr.; Freire, R. O.; Rocha, G. B.; Lima, P. P. *Eur. J. Inorg. Chem.* **2005**, *20*, 4129–4137.

(15) Biju, S.; Reddy, M. L. P.; Freire, R. O. *Inorg. Chem. Commun.* **2007**, *10*, 393–396.
 (16) (a) Xiao, M.; Selvin, P. R. *J. Am. Chem. Soc.* **2001**, *123*, 7067–7073. (b) Comby, S.; Imbert, D.; Anne-Sophie, C.; Bunzli, J. C. G.; Charvonnier, L. J.; Ziessel, R. F. *Inorg. Chem.* **2004**, *43*, 7369–7379. (c) Quici, S.; Cavazzini, M.; Marzanni, G.; Accorsi, G.; Armaroli, N.; Ventura, B.; Barigelletti, F. *Inorg. Chem.* **2005**, *44*, 529–537.
 (17) (a) Shi, M.; Li, F.; Yi, T.; Zhang, D.; Hu, H.; Huang, C. *Inorg. Chem.* **2005**, *44*, 8929–8936. (b) Xin, H.; Shi, M.; Gao, X. C.; Huang, Y. Y.; Gong, Z. L.; Nie, D. B.; Cao, H.; Bian, Z. Q.; Li, F. Y.; Huang, C. H. *J. Phys. Chem. B* **2004**, *108*, 10796–10800.

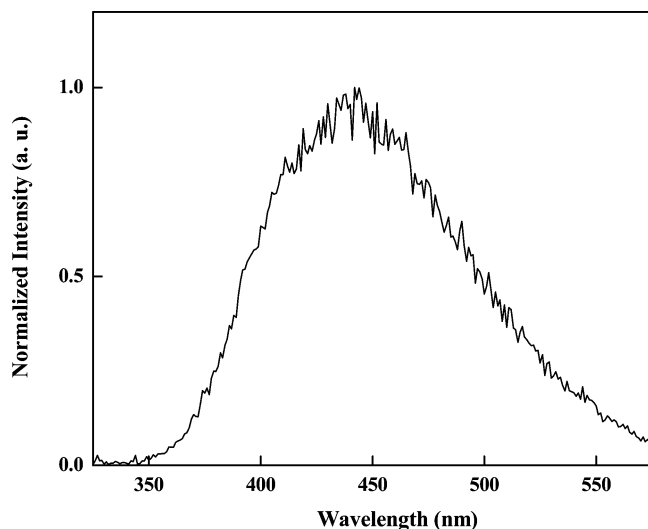


Figure 5. Phosphorescence spectrum of $Gd_2(XA)_6 \cdot 2DMSO \cdot 2H_2O$ at 77 K.

their excited singlet states, subsequent intersystem crossing of the ligands to their triplet states, and energy transfer from the triplet state to the 5D_J manifold of the Eu^{3+} ions, followed by internal conversion to the emitting 5D_0 state. Finally, the Eu^{3+} ion emits when a transition to the ground state occurs.^{14,17a} Moreover, electron transition from the higher excited states, such as 5D_3 (24 800 cm^{-1}), 5D_2 (21 200 cm^{-1}), and 5D_1 (19 000 cm^{-1}), to 5D_0 (17 500 cm^{-1}) becomes feasible by internal conversion, and most of the photophysical processes take place in this orbital. Consequently, most europium complexes give rise to typical emission bands at ~ 581 , 593, 614, 654, and 702 nm, corresponding to the deactivation of the 5D_0 excited state to the 7F_J ground states ($J = 0-4$). In a similar way, the 4f electrons of the Tb^{3+} ion are excited to the 5D_J ion manifold from the ground state. Finally, the Tb^{3+} ion emits when the 4f electrons undergo a transition from the excited-state of 5D_4 to the 7F_J ground states ($J = 6-3$). The energy-level diagram based on the present results and the possible energy transfer pathways for the lanthanide homodinuclear complexes are shown in Figure S4 (in the Supporting Information). The gap between the $^3\pi\pi^*$ and $^1\pi\pi^*$ states ($\Delta E = ^1\pi\pi^* - ^3\pi\pi^* = 6734 \text{ cm}^{-1}$) of xanthene-9-carboxylic acid is favorable for a relatively efficient intersystem crossing process.¹⁸ Latva's empirical rule¹⁹ states that an optimal ligand-to-metal energy transfer process for Ln^{3+} needs $\Delta E (^3\pi\pi^* - ^5D_J) = 2500-4000 \text{ cm}^{-1}$ for Eu^{3+}

and $2500-4500 \text{ cm}^{-1}$ for Tb^{3+} . The triplet energy level of xanthene-9-carboxylic acid (25 839 cm^{-1}) is higher than the 5D_0 level of Eu^{3+} (17 250 cm^{-1}) and the 5D_4 level of Tb^{3+} (20 400 cm^{-1}). This therefore supports the observation of stronger sensitization of the terbium complexes than the europium complexes because of the smaller overlap between the ligand triplet and europium ion excited states.

Conclusions

A series of new lanthanide complexes (Eu^{3+} , Tb^{3+} , and Gd^{3+}) of xanthene-9-carboxylic acid have been synthesized, two of which were structurally characterized. The X-ray crystal structures indicate that the Eu^{3+} and Tb^{3+} complexes are dimeric and bridged by two carboxylate ions. The coordination polyhedra can be described as distorted square antiprisms of approximately C_{2v} symmetry in which six oxygen atoms belong to the three xanthene-9-carboxylate moieties, and two oxygen atoms are provided by one water and one DMSO molecule. Interestingly, three different carboxylate coordination modes were evident at each Ln^{3+} ion. Relatively short $Ln \cdots Ln$ distances were observed in these complexes due to the presence of triply coordinated carboxylates as bridging entities. Luminescence studies demonstrated that the xanthene-9-carboxylate ligand exhibits a good antennae effect with respect to the Tb^{3+} ion due to efficient intersystem crossing ($\Delta E (^1\pi\pi^* - ^3\pi\pi^*) = 6734 \text{ cm}^{-1}$) and ligand-to-metal energy transfer. The triplet state of the xanthene-9-carboxylate ligand is located at $\sim 25 839 \text{ cm}^{-1}$, which results in a sizable sensitization of the Tb^{3+} -centered luminescence (quantum yield $7.30 \pm 0.73\%$; lifetime $1.11 \pm 0.01 \text{ ms}$), whereas the luminescence of Eu^{3+} is only poorly sensitized (quantum yield $0.06 \pm 0.01\%$; lifetime $< 10 \mu\text{s}$). Thus, the present results demonstrate that the xanthene-9-carboxylic acid complex of Tb^{3+} may find potential applications as a light conversion molecular device in many photonic applications.

Acknowledgment. The authors would like to acknowledge the financial support from Defence Research and Development Organization and University Grants Commission, New Delhi, India. The authors also wish to thank Prof. T. K. Chandrashekar, Director National Institute for Interdisciplinary Science and Technology, Trivandrum, India, for his constant encouragement and valuable discussions. A.H.C. thanks the Robert A. Welch Foundation (F-0003) for financial support.

Supporting Information Available: TG data, crystallographic data, decay profile, and energy-level diagram. This material is available free of charge via the Internet at <http://pubs.acs.org>. X-ray crystallographic information files can be obtained free of charge via www.ccdc.cam.ac.uk/conts/retrieving.html.

IC701075U

- (18) (a) Steemers, F. J.; Verboom, W.; Reinhoudt, D. N.; Vander Tol, E. B.; Verhoeven, J. W. *J. Am. Chem. Soc.* **1995**, *117*, 9408–9414. (b) Bunzli, J.-C. G.; Piguet, C. In *Encyclopedia of Materials: Science and Technology*; Buschow, K. H. J., Cahn, R. W., Flemings, M. C. B., Ilshner, B., Kramer, E. J., Mahajan, S., Eds.; Elsevier Science Ltd: Oxford, 2001; Chapter 1.10.4, pp 4465–4476.
- (19) Latva, M.; Takalo, H.; Mukkala, V. M.; Matachescu, C.; Rodriguez-Ubis, J. C.; Kanakare, J. *J. Lumin.* **1997**, *75*, 149–169.